

Probing Dense Partonic Matter at RHIC

Barbara Jacak for the PHENIX Collaboration

Department of Physics and Astronomy
Stony Brook University,
Stony Brook, NY 11794, USA

E-mail: Barbara.Jacak@stonybrook.edu

1. Introduction

Comprehensive analysis of the experimental data collected by the PHENIX experiment at the Relativistic Heavy Ion Collider (RHIC) during the first three years of operation has shown that a new state of matter is created in Au+Au collisions. This matter cannot be described in terms of ordinary color neutral hadrons [1]. Strongly interacting systems under extreme conditions of temperature and density have long been predicted to undergo a phase transition where their constituent quarks and gluons are no longer confined into hadrons.

To characterize the properties of this new matter, it is instructive to review approaches to characterize electromagnetic plasmas. Plasma physicists typically seek to determine the pressure, viscosity and equation of state, along with the thermalization time and extent of plasmas as they become experimentally accessible. It should be noted that not all electromagnetic plasmas are very long lived; the lifetime of plasmas created by high intensity laser light impinging upon a thin target is only a few nanoseconds.

These same quantities are of interest for the quark gluon plasma. They can be determined from measurements of collective behavior among particles emitted from the plasma or by probing with energetic particles transmitted through the plasma. Other plasma properties of interest for both electromagnetic and strong interaction plasmas are radiation rate, collision frequency, conductivity, opacity/transmission probability, and the Debye screening length. These are best determined using probe particles with De Broglie wavelengths short compared to the characteristic wavelength of the plasma. For electromagnetic plasmas, the probes of choice are energetic photons or electrons impinging upon the plasma from the outside. The analogous probes of the quark gluon plasma are high momentum quarks and gluons produced in the very first nucleon-nucleon collisions before the processes driving the system toward thermalization take place. In these proceedings, I will focus primarily on new measurements of such probes.

The PHENIX experiment is optimized to measure electromagnetic probes and high transverse momentum phenomena, along with global variables, multiparticle flows, and soft identified hadron spectra to understand the evolution of the produced matter over all relevant timescales. These diverse criteria required combining a large number of detection subsystems with a high bandwidth trigger and data acquisition system. A description of the PHENIX spectrometers can be found in reference [2].

2. Initial State

In order to search for effects of the matter upon the probes, it is essential to first benchmark the production of those probes in p+p collisions, and determine the effects of binding in the initial

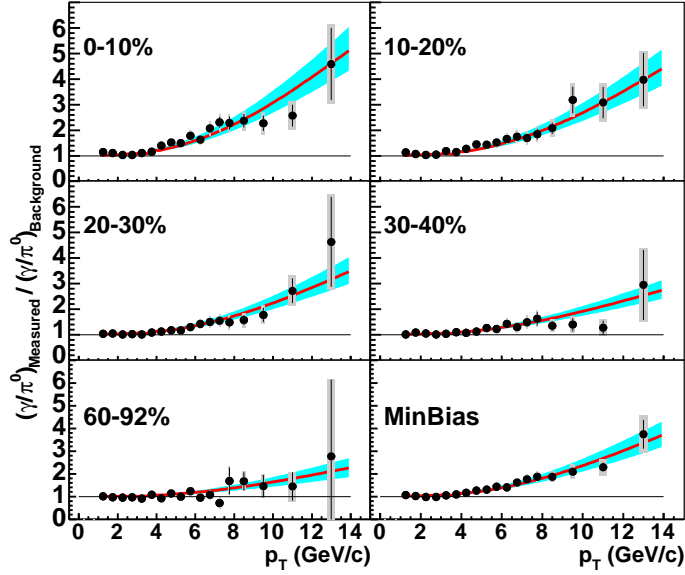


Figure 1. Double ratio of measured to background (γ/π^0) as a function of p_T for minimum bias and five centralities of Au+Au collisions at $\sqrt{s_{NN}} = 200$ GeV [6]. Solid curves are the ratio of pQCD predictions to the background photon yield based on the measured π^0 for each centrality class. The shaded regions around the curves indicate variation of the pQCD calculation for scale changes from $p_T/2$ to $2 p_T$ plus the $\langle N_{coll} \rangle$ uncertainty.

state nucleus upon the distribution of partons in the colliding nucleons. PHENIX measured the yields as a function of transverse momentum of π^0 [3] and direct photons[4] in $\sqrt{s} = 200$ GeV p+p collisions. Both the yields and the p_T distributions are well reproduced by leading order pQCD[3, 4].

As photons are not expected to interact with the color charges of quarks and gluons in the system, direct photon production in Au+Au collisions should also agree with calculations based upon pQCD. In PHENIX this expectation is tested in $\sqrt{s_{NN}} = 200$ GeV Au+Au collisions by measuring the ratio of all photons to those from π^0 decays, and plotting the double ratio of measured to simulated γ/π^0 . As the simulation is performed starting with the measured π^0 spectrum, the π^0 contribution cancels in the double ratio, making it the ratio of inclusive to direct photons. This technique minimizes systematic uncertainties. Any significant deviation of the double ratio above unity indicates a direct photon excess [5]. Figure 1 shows this double ratio as a function of p_T in Au+Au collisions in different centrality bins [6]. An excess is observed at high p_T with a magnitude that increases with increasing centrality of the collision. The measured results are compared to same NLO pQCD predictions which agreed with the PHENIX p+p data [7], scaled by the number of binary nucleon collisions for each centrality class. The binary scaled predictions agree well with the measured direct photons[6]. The increasing ratio with centrality is attributed to the decreasing decay background due to π^0 suppression [8].

The agreement of the direct photon production rate in Au+Au collisions with NLO pQCD calculations indicates that the effects of nucleons being bound inside a nucleus do not preclude the use of perturbative QCD. This is remarkable, given the complicated nuclei involved. PHENIX has also measured the production of charmed mesons in Au+Au and p+p collisions. We find that the total cross section of charmed mesons also scales with the number binary nucleon collisions [9]. As the charm mass is large, $c - \bar{c}$ pairs can only be produced in high

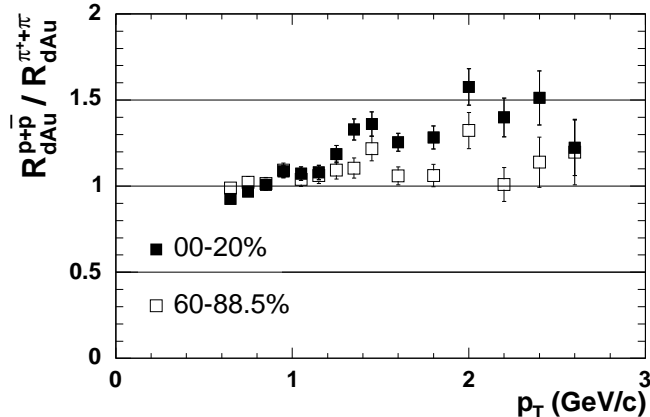


Figure 2. Ratio of the proton over the pion nuclear modification in d+Au collisions for central and peripheral events. Error bars indicate statistical errors only.

momentum transfer collisions, and should therefore be calculable with pQCD. The photon results suggest that binary collision scaling should hold for charm production as well, and PHENIX has established that it does.

Several initial state effects may be expected in collisions involving nuclei. These include nuclear shadowing, saturation of the gluon distribution, and multiple initial state scattering of the incoming partons. The collision scaling of high p_T photons and charm yields indicate that these effects mostly cancel for large q^2 processes at mid-rapidity. However, they should be more important for softer processes and at rapidities nearer those of the beams. A wide range of d+Au collision data was collected to quantify these effects. PHENIX can probe saturation effects via the rapidity dependence of hadron production, and initial state multiple scattering via the dependence of hadrons upon the number of collisions suffered by each deuteron participant. We find that calculations incorporating shadowing and initial state semi-hard scattering can reproduce the data on hadron production at midrapidity reasonably well [10].

However, no model of initial state multiple scatterings can predict the difference in baryon and meson yields in nucleon- or deuteron- nucleus collisions. Baryon yields at moderate p_T are considerably enhanced in central d+Au collisions compared to p+p. This contrasts with the very small enhancement observed for pions, and is illustrated in Figure 2. The figure shows the ratio of R_{dAu} for baryons to that of mesons in the most peripheral (60-88.5%) and most central (0-20%) d+Au collisions. The nuclear modification factor, R_{dAu} is defined as

$$R_{dAu} = \frac{(1/N_{dAu}^{evt})d^2 N_{dAu}/dydp_T}{T_{dAu}d^2\sigma_{inel}^{pp}/dydp_T},$$

where $T_{dAu} = \langle N_{coll} \rangle / \sigma_{inel}^{pp}$ describes the nuclear geometry and $d^2\sigma_{inel}^{pp}/dydp_T$ for p+p collisions is derived from the measured p+p cross section. $\langle N_{coll} \rangle$ is the average number of inelastic nucleon-nucleon collisions determined from a Glauber simulation. The figure shows that the difference between baryons and mesons reaches 50% in central collisions. More successful explanations of the baryon enhancement invoke hadronization by recombination of quarks from fragmenting jets with those drawn from the nearby nuclear medium [11].

The rapidity dependence of charged hadron production in d+Au collisions is measured by PHENIX using the muon arms, which cover $\eta = 1.4 - 2.2$. We detect stopped muons from hadron

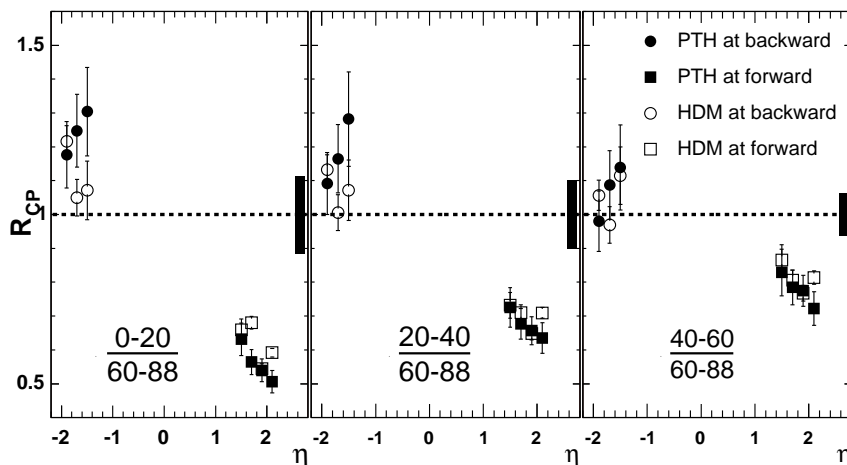


Figure 3. R_{cp} as a function of η for $1.5 \langle p_T \rangle$ 4.0 GeV/c for different centrality classes.

decays and also hadrons which punch through the absorber and interact in the muon arm [12]. As comparable data from p+p collisions are as yet unavailable, we calculate a nuclear modification factor by comparing yields in central and peripheral collisions, scaled by the corresponding number of binary nucleon collisions in each centrality bin, $\langle N_{coll} \rangle$:

$$R_{cp} = \frac{\langle \left(\frac{dN}{d\eta dp_T} \right)^{Central} \rangle / \langle N_{coll}^{Central} \rangle}{\langle \left(\frac{dN}{d\eta dp_T} \right)^{Peripheral} \rangle / \langle N_{coll}^{Peripheral} \rangle}$$

R_{cp} integrated in the p_T range from 1.5 to 4.0 GeV/c is shown in Figure 3 as a function of η for the different centrality classes [13]. We observe that R_{cp} shows a suppression at forward rapidity (deuteron going direction) that is largest for the most central events. The opposite trend is observed at backward rapidity (Au going direction), where R_{cp} shows an enhancement that is also largest for the most central events. There is a weak p_T dependence, with slightly smaller R_{cp} at lower p_T . We observe a clear pseudorapidity dependence at forward rapidity with R_{cp} dropping further at larger η values; our results are consistent with the BRAHMS data [14]. Within the uncertainties, we are unable to discern any pseudorapidity dependence at the backward rapidity. Forward suppression is qualitatively consistent with several theories including shadowing or saturation effects in initial state multiple scattering, but also recombination [15, 16, 17]. The enhancement at backward rapidity has not yet been explained.

3. Thermalization

Turning now from the initial state, I discuss observables that tell about the approach to thermalization in Au+Au collisions. PHENIX measures many species of hadrons, including the ϕ meson via its decays to K^+K^- and e^+e^- . We find that the slope of the ϕ p_T distributions reconstructed in the two decay channels are consistent with each other, and are also consistent with a blast wave fit to π, K , and p spectra [18]. This observation supports the picture of a common expanding source for all low and intermediate momentum hadrons at midrapidity.

Good tests of the system's approach toward thermalization are the magnitude and species dependence of the elliptic flow. Elliptic flow is measured by Fourier analysis of the momentum distribution of emitted particles as a function of the azimuthal angle with respect to the plane of the Au+Au collision. The strength of the flow is quantified by the magnitude of the second

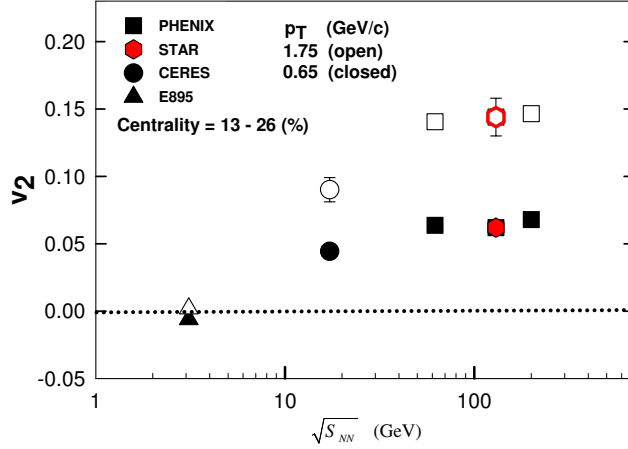


Figure 4. Differential v_2 vs. $\sqrt{s_{NN}}$ for charged hadrons in nucleus-nucleus collisions. Results are shown for a centrality class of 13-26% and p_T of 1.75 GeV/c (open symbols) and 0.65 GeV/c (closed symbols).

harmonic coefficient of the Fourier expansion, generally known as the v_2 parameter. PHENIX has measured v_2 for charged pions, kaons, protons, antiprotons, neutral pions, inclusive photons and electrons from the decay of charmed mesons. This is measured using several methods, including two particle correlations at midrapidity, two-particle cumulants, and the distribution of particles in the central arm with respect to the reaction plane determined by the beam-beam counters (BBC) at rapidity $\eta = 3.0 - 3.9$. Most of the measurements for identified particles use the PHENIX central arm spectrometers and the BBC reaction plane. We find that the different species exhibit approximately the same v_2 per constituent quark. v_2 rises as a function of p_T up to 1.5-2 GeV/c per constituent quark, then falls again at higher p_T . In $\sqrt{s_{NN}} = 62.4$ GeV Au+Au collisions, the observed v_2 per quark is quite similar to that in 200 GeV Au+Au collisions.

This is illustrated in Figure 4, which shows v_2 for inclusive charged hadrons at two p_T values (0.65 and 1.75 GeV/c), as a function of \sqrt{s} for heavy ion collisions from AGS through RHIC energies [19]. The data are compared for relatively central collisions representing the upper 13-26% of the total cross section. For both p_T cuts, the magnitude of v_2 shows a significant increase with collision energy ($\approx 50\%$ increase from SPS to RHIC) up to $\sqrt{s_{NN}} = 62.4$ GeV. Thereafter, v_2 appears to saturate for larger beam energies. Given the fact that the energy density is estimated to increase by approximately 30% over the range $\sqrt{s_{NN}} = 62.4 - 200$ GeV, this apparent saturation of v_2 may be indicative of the role of a rather soft equation of state. Such a softening could result from the production of mixed phase within this energy range.

Of course, for such a discussion to be applicable, the system must be in local thermal equilibrium. For thermalization to occur, the particles must interact and/or radiate. If such processes occur with sufficient frequency, the system should be describable by locally equilibrated fluid elements, with a velocity profile following $\beta_{\parallel}^{Fluid} = z/t$. This has been tested by calculations with hydrodynamical models of Au+Au collisions with initial conditions fixed by the collision geometry and energy density fixed by total particle and energy production; for more detail see discussion and references in [1]. In a hydrodynamic picture, the source of elliptic flow is the spatial anisotropy of the energy density in the transverse plane at the time hydrodynamics becomes valid (i.e. at the time that local thermal equilibrium is reached). If local equilibration

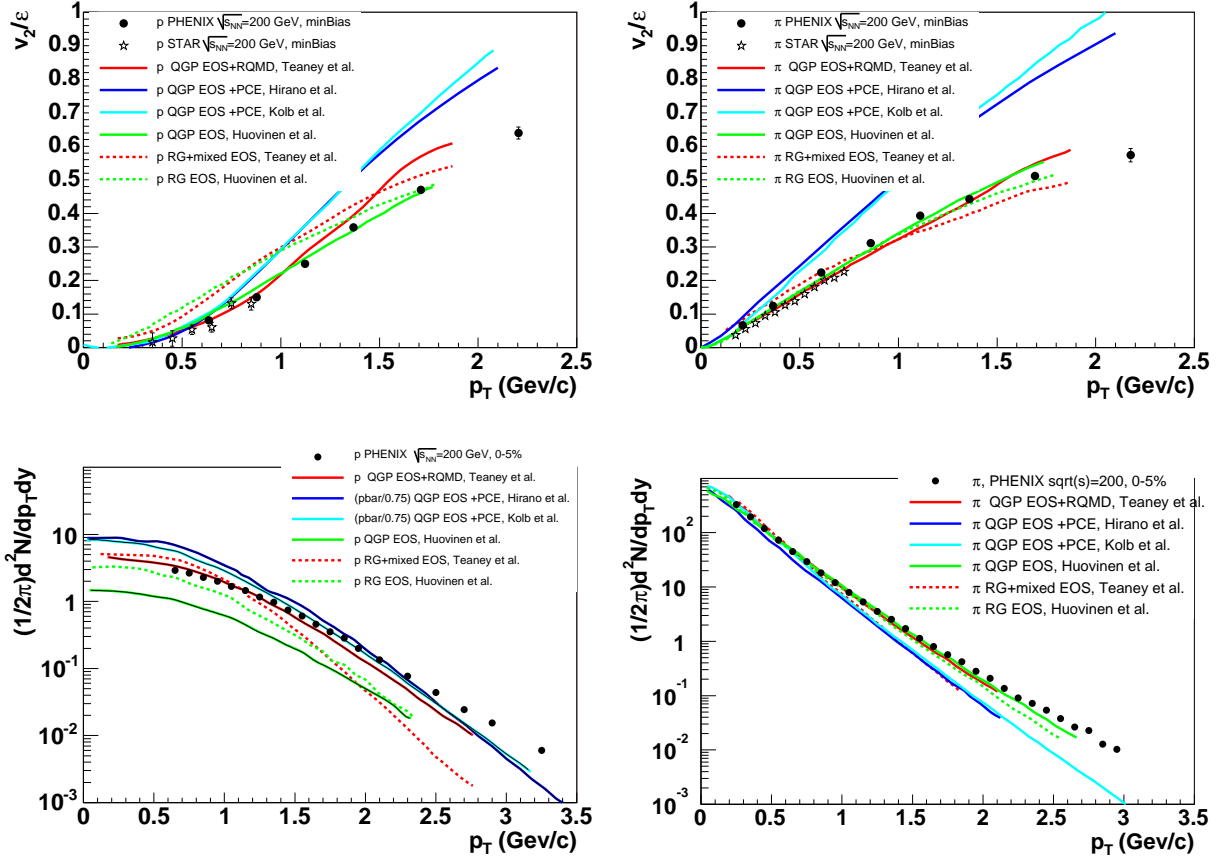


Figure 5. Top panels: proton and pion $1/\epsilon v_2(p_T)$ vs. p_T for minimum bias collisions at RHIC, compared with hydrodynamics calculations. Bottom panels: proton and pion p_T spectra for the most central (0-5%) collisions at RHIC compared with the same hydrodynamics calculations. See text and [1] for references to the data and hydrodynamics calculations.

and the onset of hydrodynamical behavior is delayed because interactions between the initially produced particles are weak at first, then the spatial anisotropy giving rise to elliptic flow is reduced. Consequently, the magnitude of the v_2 parameter is sensitive to the thermalization time. The thermalization time may be inferred from the hydrodynamics calculations constrained with data on the p_T and species dependence of elliptic flow and particle spectra.

Figure 5 shows the comparison of a number of hydrodynamics models [20, 21, 22, 23] with the data on pion and proton v_2 as a function of p_T for minimum bias Au+Au collisions, and pion and proton p_T spectra in central collisions [1]. The calculations including a phase transition from QGP to a hadronic phase are shown with solid lines, while calculations with no pure QGP phase are drawn with dashed lines. The four calculations that include a QGP phase all assume an ideal gas EOS for the QGP phase, a resonance gas for the hadronic phase, and connect the two using a first-order phase transition and a Maxwell construction. The calculations that do not include a QGP phase either have a hadronic plus mixed phase with the latent heat of the transition forced to infinity (Teaney)[20], or they use only a hadronic resonance gas (i.e. no mixed or QGP phases in one of Huovinen's calculations) [21]. The calculations also differ in their treatment of the final hadronic phase and freezeout. Hirano's [22] is the only 3D hydrodynamics calculation; this and

Kolb's [23] both allow for partial chemical equilibrium by chemically freezing out earlier than the kinetic freezeout. This has been done in order to reproduce the large proton yield measured at RHIC. In contrast, Huovinen[21] maintains full chemical equilibrium throughout the hadronic phase. Teaney[20] uses a hybrid model that couples the hadronic phase to RQMD to allow hadrons to freeze out according to their scattering cross sections; incorporating this step allows for chemical equilibrium to be broken in the hadronic phase. All four models have assumed ideal hydrodynamics, i.e. zero viscosity and zero mean free path.

From the top panels of Figure 5 it is clear that the four calculations that include a phase transition from the QGP phase to a hadronic phase (solid lines) reproduce the low p_T proton data better than the two hydro calculations without the QGP phase (dashed lines). The presence of a first order phase transition softens the equation of state, reducing the elliptic flow. At higher p_T there is quite some variation between the models. Part of this is due to the modeling of the final hadronic stage. It is notable that Kolb's and Hirano's calculations significantly overpredict v_2 , and they both have similar partial chemical equilibrium assumptions in the late hadronic stage. Comparing to the transverse momentum spectra, we see that all the models reproduce the pion spectra below 1 GeV/c p_T . Calculations including a QGP phase do a better job reproducing the proton spectra, presumably because of increased transverse flow from the stronger early pressure gradients. The calculations with partial chemical equilibrium during the hadronic phase overpredict the proton spectra at low p_T .

All the models qualitatively reproduce the trends observed in the data, but significant sensitivity to the assumptions in the models is demonstrated. Thus it is important to reduce the model uncertainty in the final state to extract quantitative information on the equation of state during the reaction, including the possible softening of the equation of state due to the presence of a mixed phase. Nevertheless, we can use the calculations to extract limits for the thermalization time[1]. All the hydrodynamical models require quite short thermalization times, in the range of 0.6-1.0 fm/c, to reproduce the magnitude of the observed elliptic flow.

The general success of hydrodynamics models to explain the data provides strong evidence for local thermalization of the system, or at least for equipartition of the momenta, in the early stage of the collision. It is natural to ask whether the heavy quarks flow along with the light ones, or whether their large masses increase the time required for them to thermalize so much that they cannot receive the same velocity boost from the collective motion as the light quarks.

Electrons are a useful tool for the study of heavy quarks such as charm and bottom. PHENIX has measured single electron p_T spectra in Au+Au collisions at $\sqrt{s_{NN}} = 130$ GeV[24] and 200 GeV[9]. The results are consistent with semileptonic charm decays in addition to the decays of light mesons and photon conversions. The spectrum of electrons of non-photonic origin can be measured by adding a converter of well-calibrated thickness to determine the photonic electron rate and subtracting these from the inclusive electron spectrum. Alternatively, the measured π^0 and η spectra can be used to calculate the photonic sources of electrons, including conversions of photons from light meson decays. The calculated background spectrum is then subtracted from the measured electrons. The former technique was used in [9], and the latter to measure charm production in p+p collisions. We use the same approach to determine v_2 for open charm by measuring the distribution of electrons with respect to the reaction plane. Though electrons originating from decays of D mesons have a significant angular deviation from the original D meson directions, the extracted v_2 value remains well correlated with the v_2 of the D meson[25]. Consequently, PHENIX uses electrons and positrons to determine v_2 for heavy quarks. We subtract v_2 of electrons from photon conversions and Dalitz decays of light neutral mesons from the inclusive electron v_2 [26].

Figure 6 shows the heavy flavor v_2 in minimum bias $\sqrt{s_{NN}} = 200$ GeV Au+Au collisions. The statistical error bars are propagated from the statistical uncertainties on the inclusive electron v_2 , while the bands show the 1σ systematic uncertainty of the heavy flavor v_2 . The result allows

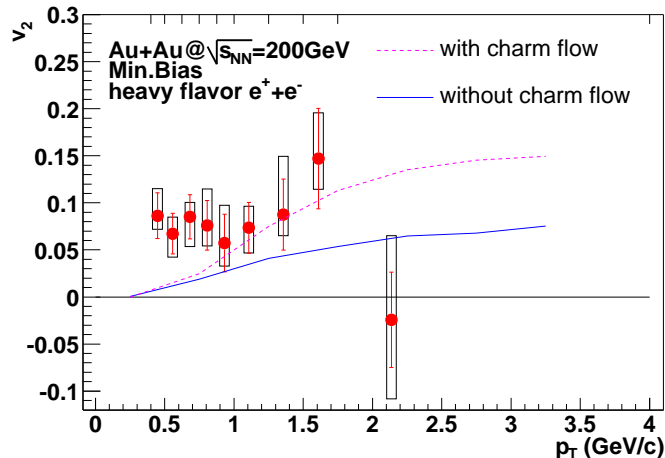


Figure 6. Elliptic flow (v_2) for electrons and positrons from heavy flavor decays, as a function of the electron or positron p_T , in minimum bias $\sqrt{s_{NN}} = 200$ GeV Au+Au collisions. The lines correspond to calculations with two different charm flow scenarios[25]. The solid line has no rescattering of the initially produced charm quarks (i.e. no charm flow), while the dashed line reflects the effect of complete thermalization (maximum charm flow).

calculation of the confidence level for a non-zero v_2 , yielding 90% confidence that the heavy flavor electron v_2 is non-zero in the p_T range from 1 - 1.75 GeV/c. The v_2 of electrons from decays of D mesons have been predicted assuming that the D mesons are formed by charm quark coalescence with thermal light quarks. The solid line on Figure 6 assumes that the charm and anticharm quarks experience no reinteractions after they are formed in initial state hard processes. The second scenario, shown by the dashed line, assumes complete thermalization of the heavy quarks with the transverse flow of the bulk matter. Though the large statistical errors on this data sample do not allow exclusion of either scenario, the points do suggest that heavy quark flow may indeed be taking place.

4. Probes of the Partonic State

Given the various pieces of evidence pointing toward early local thermalization of the system, it is of great interest to use the short wavelength probes discussed in the Introduction to measure the properties of the hot, dense matter ≈ 1 fm/c after the Au nuclei traverse one another. Of paramount interest is how the probes couple to the medium. It is already well established that hard scattered partons traversing the medium experience considerable energy loss[27]. But the exact nature of the interaction of the parton with the medium is not well studied experimentally. This question is particularly interesting for partons of moderate p_T , between 5 and 10 GeV/c, which may begin to hadronize in or near the medium.

Having seen the tantalizing result that heavy quarks may indeed flow along with the bulk of light quarks, it is natural to wonder whether heavy quarks lose energy in the medium as the light quarks do. It has been predicted that the energy loss of charm quarks should be less than that of light quarks, as the large charm quark mass decreases the phase space available for gluon radiation (i.e. "dead cone" effect)[28]. The dead cone should be even more significant for bottom quarks. More detailed calculations include also simulation of the effects of the charm p_T spectral shape and contributions from B meson decays; these predict that the nuclear modification factor for electrons from charm decays should be 0.6-0.8 for electrons with

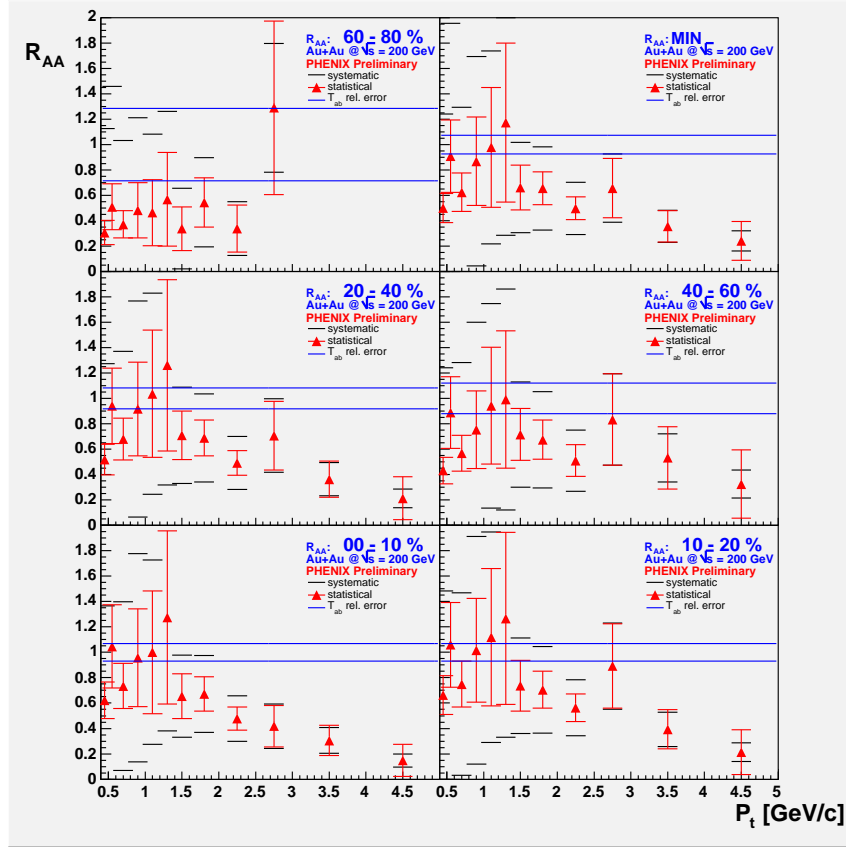


Figure 7. Nuclear modification factor, R_{AA} , for electrons and positrons from heavy quark decays in $\sqrt{s_{NN}} = 200$ GeV Au+Au collisions. The error bars show statistical errors, while the bands around each point indicate systematic uncertainties. The bands centered about $R_{AA} = 1.0$ indicate the systematic uncertainty in the number of binary nucleon collisions in each centrality class.

$p_T \approx 2.5$ GeV/c [29]. This is a significant suppression, though less than that observed for light quarks[27, 8]. Armesto and co-workers take into account differences between the energy loss of quarks and gluons traversing the medium, and predict even larger suppression of electrons from heavy quarks[30]. Moore and Teaney point out that if the charm quarks demonstrate flow along with the bulk of the medium, this is evidence for thermalization of charm, and then the medium modifications of the charm spectrum should be substantial[31].

Figure 7 shows the nuclear modification factor, R_{AA} for electrons and positrons from heavy quark decays in $\sqrt{s_{NN}} = 200$ GeV Au+Au collisions, as a function of the electron p_T . The figure shows minimum bias collisions in addition to 5 centrality classes. Electrons from heavy quark decays are measured by subtracting the p_T spectrum of electrons from photonic sources, calculated using the measured π^0 spectra, from the inclusive electron spectrum. The same subtraction technique is used for Au+Au and reference p+p spectra, but of course the input π^0 spectra are different. In the most peripheral collisions, statistical uncertainties limit the accessible p_T range, but where there are data, all the points are consistent with $R_{AA} = 1$, i.e. no suppression. In more central collisions, R_{AA} falls well below 1.0 for electron $p_T \geq 2$ GeV/c, providing clear evidence for charm energy loss. At the highest p_T of this measurement, the electron R_{AA} becomes nearly as small as that for π^0 . This is remarkable, as electrons above

3.5 or 4.0 GeV/c p_T are expected to also include contributions from B meson decays, and B mesons should experience less energy loss than D mesons. Though the data are consistent with predictions from Armesto et al.[30] for medium densities at the extreme high end of those allowed by the observed light quark energy loss, the lack of observable dilution from B meson decays is intriguing.

Hard scattered partons are formed in the initial nucleon collisions, and traverse the hot, dense medium. These partons experience significant energy loss via medium-induced gluon radiation. The next question is - where does the radiated energy go? Though radiated gluons are nearly collinear with the parent parton, they are rather soft and may interact further with the gluon field in the medium. Though it is often assumed that fragmentation takes place outside the medium, the formation time for 2-4 GeV/c p_T hadrons is not very long, particularly for baryons. Thus fragmentation may begin in or near the medium and involve not only the quarks and antiquarks from gluons radiated as fragmentation begins, but also comoving gluons from medium-induced radiation, and indeed recombination of jet partons with partons from the medium itself[11].

PHENIX probes these processes using correlations of high transverse momentum particles, in the p_T range from 1 - 4 GeV/c. We select Au+Au collisions containing hard scattering events by requiring detection of a hadron with $2.5 \leq p_T \leq 4$ GeV/c. We then construct correlation functions between these trigger particles and associated particles with $1.0 \leq p_T \leq 2.5$ GeV/c, as a function of their azimuthal angle difference[32, 33]. We correct for the non-uniform PHENIX azimuthal acceptance by constructing an area normalized correlation function utilizing pairs from mixed events. To extract the yield of jet-induced pairs, we analyze the correlation function assuming that each hadron can be attributed either to a jet fragmentation source or to the underlying event. The underlying event has an azimuthal correlation arising from the fact that the single particle distributions respect the reaction plane of the event. This correlation is removed by modulating the background pair distribution with the inclusive v_2 value measured for the trigger and associated particle p_T range. Thus the correlation function is decomposed via

$$C(\Delta\phi) = b_0(1 + 2\langle v_2^T v_2^A \rangle \cos(2\Delta\phi)) + J(\Delta\phi)$$

The average level of the background, b_0 is fixed by assuming that the jet fragmentation yield of particle pairs is zero for at least one value of $\Delta\phi$. We refer to this as the ZYAM (zero yield at minimum) assumption. We have verified the validity of this assumption by independently estimating the b_0 values using the T*A combinatorial pair rate. Once the background level is determined, we extract conditional yields for particle pairs from jets.

The conditional yields of jet partners per trigger particle are shown in Figure 8[33]. For the most peripheral event sample, the jet associated yield distribution has the same shape as jet pairs in p+p collisions: a well-defined near side peak around $\Delta\phi = 0$ and a somewhat wider away side peak around $\Delta\phi = \pi$. For more central event samples, the shape of the near-side peak is essentially unchanged while the associated yield in the near-side peak increases, indicating some change in the fragmentation process. A much more dramatic change is visible in the away side peak, which is considerably broader in all the centrality classes more central than 60%. In mid-central and central collisions there is a local minimum at $\Delta\phi = \pi$. Though the existence of these local minima *per se* is not significant once we take the systematic errors on $\langle v_2^T v_2^A \rangle$ into account, it is clear that the away side peak in more central collisions has a very different shape than in peripheral collisions.

Convoluting the jet fragments' angles with respect to their parent partons and the acoplanarity between the two partons would yield a Gaussian-like shape in $\Delta\phi$, possibly broadened through jet quenching. The observed shapes in the away side peaks cannot result from such a convolution. The away side peaks are suggestive of recent theoretical predictions of dense medium effects on fragment distributions. These include combination of jet partons with medium partons accelerated by a density wave in the shocked medium[34, 35, 36], and jet

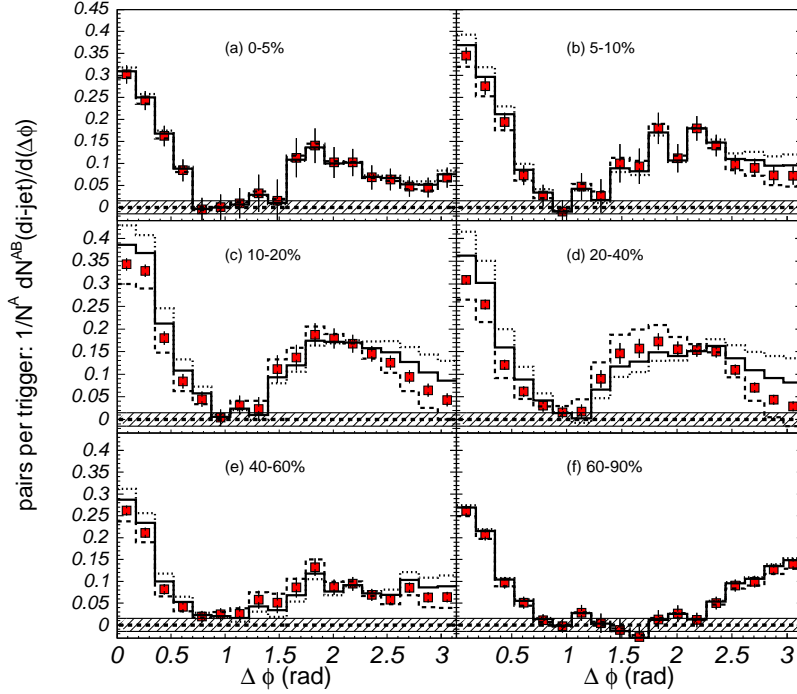


Figure 8. Jet fragment pair relative azimuthal angle distributions for different centralities in $\sqrt{s_{NN}} = 200$ GeV Au+Au collisions[33]. The yields are normalized per trigger particle. The shaded bands indicate the systematic error associated with the determination of the relative angle where the jet pair yield is zero. The dashed(solid) lines are the distributions that would result from increasing (decreasing) $\langle v_2^T v_2^A \rangle$ by one unit of the systematic error; the dotted curve would result from decreasing by two units.

asymmetries caused by the hydrodynamic flow of the underlying event[37]. The broadening of the away side jet implies that integration of the away side peak in a narrow angular range around $\Delta\phi = \pi$ yields fewer associated partners in central collisions than in peripheral Au+Au or in d+Au collisions. However, integrating over the entire broadened peak recovers the jet partners in the range $1.0 \text{ GeV}/c \leq p_T^A \leq 2.5 \text{ GeV}/c$ used in this analysis.

5. Summary

The PHENIX collaboration has measured a large number of observables in Au+Au, d+Au and p+p collisions at RHIC. We have shown that direct photons and hard processes are calculable with perturbative QCD, yielding a calibrated source of short wavelength probes of the medium formed in nuclear collisions. Anomalous behavior of baryon yields is seen in d+Au collisions, suggesting that baryon formation is already subject to the influence of the nearby nucleus in that case.

The elliptic flow trends support the picture of rapid thermalization in Au+Au collisions. Furthermore, there are first indications that heavy quarks may participate in the collective flow with the light quarks. We have seen that heavy quarks lose energy in the hot dense medium, as may be expected if they approach local thermal equilibrium. Jet fragmentation is modified in

central and semi-central Au+Au collisions. The data suggest that the lost energy may excite the medium and modify the formation of jet hadrons. The formation of moderate p_T baryons (from approximately 2-5 GeV/c) is expected to take place in, or near, the medium in Au+Au and d+Au collisions. Indeed the data show enhanced baryon production probability in both cases. This suggests that recombination of partons from the fragmenting jet and from the medium play an important role in hadronization.

Quantitative determination of the opacity of and collision frequency in the medium, along with its color Debye screening length awaits completion of the analysis of the high statistics run4 data. PHENIX has a billion events currently being analyzed.

6. References

- [1] K. Adcox, *et al.* Nucl. Phys. **A757**, 184 (2005).
- [2] K. Adcox *et al.*, Nucl. Instrum. Methods **A499**, 469 (2003) and references therein.
- [3] S.S. Adler *et al.*, Phys. Rev. Lett. **91**, 241803 (2003).
- [4] S.S. Adler *et al.*, Phys. Rev. D **71**, 071102R (2005).
- [5] See talk of S. Bathe, these proceedings.
- [6] S.S. Adler *et al.*, Phys. Rev. Lett. **94**, 232301 (2005).
- [7] L.E. Gordon and W. Vogelsang, Phys. Rev. D **48**, 3136 (1993).
- [8] S.S. Adler *et al.*, Phys. Rev. Lett. **91**, 072301 (2003).
- [9] S.S. Adler *et al.*, Phys. Rev. Lett. **94**, 082301 (2005).
- [10] A. Accardi and M. Gyulassy, Phys. Lett. **B586**, 244 (2004).
- [11] R. Hwa and C.B. Yang, Phys. Rev. C **70**, 037901 (2004).
- [12] See talk of A. Purwar, these proceedings.
- [13] S. S. Adler *et al.*, Phys. Rev. Lett. **94**, 082302 (2005).
- [14] I. Arsene *et al.*, Phys. Lett. **B595**, 209 (2004).
- [15] D. Kharzeev, Y.V. Kovchegov and K. Tuchin, arXiv:hep-ph/0405045.
- [16] R. Vogt, arXiv:hep-ph/0405060.
- [17] R. Hwa, C.B. Yang and R.J. Fries, arXiv:nucl-th/0410111.
- [18] S. S. Adler *et al.*. arXiv:nucl-ex/0410012 (accepted in Phys. Rev. C).
- [19] S. S. Adler *et al.*. Phys. Rev. Lett. **94**, 232302 (2005).
- [20] D. Teaney, J. Lauret, E.V. Shuryak, arXiv:nucl-th/0110037.
- [21] P. Huovinen, P.F. Kolb, U.W. Heinz, P.V. Ruuskanen, and S.A. Voloshin, Phys. Lett. **B503**, 58 (2001).
- [22] T. Hirano and K. Tsuda, Phys. Rev. C **66**, 054905 (2002).
- [23] P. Kolb and U. Heinz, arXiv:nucl-th/0305084 and "Quark Gluon Plasma 3", Editors R.C. Hwa and X.N. Wang, World Scientific, Singapore.
- [24] K. Adcox *et al.*. Phys. Rev. Lett. **88**, 082301 (2002).
- [25] V. Greco, C.M. Ko and R. Rapp, Phys. Lett. **B595**, 202 (2004).
- [26] S. S. Adler *et al.*. arXiv:nucl-ex/0503003.
- [27] K. Adcox *et al.*. Phys. Rev. Lett. **88**, 022301 (2002).
- [28] D. Kharzeev and Y. Dokshitzer, Phys. Lett. **B519**, 199 (2001).
- [29] M. Djordjevic, M. Gyulassy and S. Wicks, arXiv:hep-ph/0410372.
- [30] N. Armesto, S. Dainese, C. Salgado, and U. Wiedemann, arXiv: hep-ph/0501225.
- [31] Guy Moore and Derek Teaney, arXiv:hep-ph/0412346.
- [32] See talk of N. Ajitanand, these proceedings.
- [33] S.S. Adler, *et al. et al.*. arXiv:nucl-ex/0507004.
- [34] J. Casalderrey-Solana, E.V. Shuryak and D. Teaney, arXiv:hep-ph/0411315.
- [35] H. Stoecker, Nucl. Phys. **A750**, 121 (2005).
- [36] J. Ruppert and B. Muller, arXiv:hep-ph/0503158.
- [37] N. Armesto, C. Salgado and U. Wiedemann, arXiv:hep-ph/0411341.